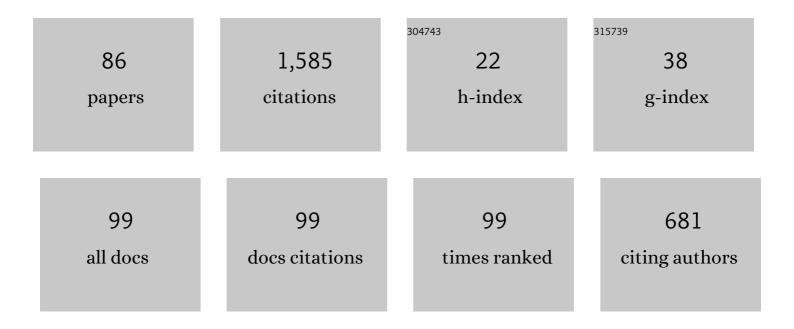
Beatriz Quintal

List of Publications by Year in descending order

Source: https://exaly.com/author-pdf/820245/publications.pdf Version: 2024-02-01



#	Article	IF	CITATIONS
1	Quasi-static finite element modeling of seismic attenuation and dispersion due to wave-induced fluid flow in poroelastic media. Journal of Geophysical Research, 2011, 116, .	3.3	148
2	Measurements of seismic attenuation and transient fluid pressure in partially saturated Berea sandstone: evidence of fluid flow on the mesoscopic scale. Geophysical Journal International, 2013, 195, 342-351.	2.4	103
3	Synchrotron-based X-ray tomographic microscopy for rock physics investigations. Geophysics, 2013, 78, D53-D64.	2.6	88
4	Low-frequency reflections from a thin layer with high attenuation caused by interlayer flow. Geophysics, 2009, 74, N15-N23.	2.6	77
5	Seismic attenuation in partially saturated Berea sandstone submitted to a range of confining pressures. Journal of Geophysical Research: Solid Earth, 2016, 121, 1664-1676.	3.4	63
6	Sensitivity of S-wave attenuation to the connectivity of fractures in fluid-saturated rocks. Geophysics, 2014, 79, WB15-WB24.	2.6	62
7	Pore fluid effects on S-wave attenuation caused by wave-induced fluid flow. Geophysics, 2012, 77, L13-L23.	2.6	55
8	Bubbles attenuate elastic waves at seismic frequencies: First experimental evidence. Geophysical Research Letters, 2015, 42, 3880-3887.	4.0	55
9	Laboratoryâ€based seismic attenuation in Fontainebleau sandstone: Evidence of squirt flow. Journal of Geophysical Research: Solid Earth, 2015, 120, 7526-7535.	3.4	54
10	Laboratory measurements of seismic attenuation in sandstone: Strain versus fluid saturation effects. Geophysics, 2014, 79, WB9-WB14.	2.6	53
11	An overview of laboratory apparatuses to measure seismic attenuation in reservoir rocks. Geophysical Prospecting, 2014, 62, 1211-1223.	1.9	53
12	Numerical homogenization of mesoscopic loss in poroelastic media. European Journal of Mechanics, A/Solids, 2015, 49, 382-395.	3.7	47
13	A simple hydromechanical approach for simulating squirt-type flow. Geophysics, 2016, 81, D335-D344.	2.6	45
14	Seismic Attenuation and Stiffness Modulus Dispersion in Porous Rocks Containing Stochastic Fracture Networks. Journal of Geophysical Research: Solid Earth, 2018, 123, 125-143.	3.4	45
15	Impact of fluid saturation on the reflection coefficient of a poroelastic layer. Geophysics, 2011, 76, N1-N12.	2.6	44
16	Frequency-dependent attenuation as a potential indicator of oil saturation. Journal of Applied Geophysics, 2012, 82, 119-128.	2.1	44
17	Forced oscillation measurements of seismic wave attenuation and stiffness moduli dispersion in glycerineâ€saturated Berea sandstone. Geophysical Prospecting, 2019, 67, 956-968.	1.9	33
18	Attenuation mechanisms in fractured fluidâ€saturated porous rocks: a numerical modelling study. Geophysical Prospecting, 2019, 67, 935-955.	1.9	32

#	Article	IF	CITATIONS
19	Numerical modeling and laboratory measurements of seismic attenuation in partially saturated rock. Geophysics, 2014, 79, L13-L20.	2.6	28
20	Seismic attenuation in partially saturated rocks: Recent advances and future directions. The Leading Edge, 2014, 33, 640-646.	0.7	28
21	Frequency-dependent attenuation and dispersion caused by squirt flow: Three-dimensional numerical study. Geophysics, 2020, 85, MR129-MR145.	2.6	26
22	Frequency scaling of seismic attenuation in rocks saturated with two fluid phases. Geophysical Journal International, 2017, 208, 221-225.	2.4	25
23	Numerically quantifying energy loss caused by squirt flow. Geophysical Prospecting, 2019, 67, 2196-2212.	1.9	22
24	Numerical upscaling of frequencyâ€dependent P―and Sâ€wave moduli in fractured porous media. Geophysical Prospecting, 2016, 64, 1166-1179.	1.9	21
25	Representative elementary volumes for evaluating effective seismic properties of heterogeneous poroelastic media. Geophysics, 2016, 81, D169-D181.	2.6	20
26	Seismic Wave Attenuation and Dispersion Due to Partial Fluid Saturation: Direct Measurements and Numerical Simulations Based on Xâ€Ray CT. Journal of Geophysical Research: Solid Earth, 2021, 126, e2021JB021643.	3.4	19
27	Seismic attenuation and dispersion in poroelastic media with fractures of variable aperture distributions. Solid Earth, 2019, 10, 1321-1336.	2.8	18
28	Integrated numerical and laboratory rock physics applied to seismic characterization of reservoir rocks. The Leading Edge, 2011, 30, 1360-1367.	0.7	17
29	Numerical modeling of fluid effects on seismic properties of fractured magmatic geothermal reservoirs. Solid Earth, 2017, 8, 255-279.	2.8	17
30	Numerical simulation of ambient seismic wavefield modification caused by pore-fluid effects in an oil reservoir. Geophysics, 2013, 78, T41-T52.	2.6	14
31	Squirt Flow in Cracks with Rough Walls. Journal of Geophysical Research: Solid Earth, 2020, 125, e2019JB019235.	3.4	14
32	Seismic lowâ€frequency anomalies in multiple reflections from thinly layered poroelastic reservoirs. , 2007, , .		13
33	An analytical study of seismoelectric signals produced by 1-D mesoscopic heterogeneities. Geophysical Journal International, 2015, 201, 329-342.	2.4	13
34	Squirt flow due to interfacial water films in hydrate bearing sediments. Solid Earth, 2018, 9, 699-711.	2.8	13
35	Fully-automated adaptive mesh refinement for media embedding complex heterogeneities: application to poroelastic fluid pressure diffusion. Computational Geosciences, 2020, 24, 1101-1120.	2.4	13
36	Azimuth-, angle- and frequency-dependent seismic velocities of cracked rocks due to squirt flow. Solid Earth, 2020, 11, 855-871.	2.8	13

#	Article	IF	CITATIONS
37	Resolving Wave Propagation in Anisotropic Poroelastic Media Using Graphical Processing Units (GPUs). Journal of Geophysical Research: Solid Earth, 2021, 126, e2020JB021175.	3.4	12
38	Imperialist competitive algorithm optimization method for nonlinear amplitude variation with angle inversion. Geophysics, 2019, 84, N81-N92.	2.6	11
39	The Effect of Boiling on Seismic Properties of Waterâ€Saturated Fractured Rock. Journal of Geophysical Research: Solid Earth, 2017, 122, 9228-9252.	3.4	10
40	An accurate analytical model for squirt flow in anisotropic porous rocks — Part 1: Classical geometry. Geophysics, 2022, 87, MR85-MR103.	2.6	10
41	Numerical analysis of local strain measurements in fluid-saturated rock samples submitted to forced oscillations. Geophysics, 2018, 83, MR309-MR316.	2.6	9
42	Identification of viscoelastic properties from numerical model reduction of pressure diffusion in fluid-saturated porous rock with fractures. Computational Mechanics, 2019, 63, 49-67.	4.0	9
43	Digital rock physics applied to squirt flow. Geophysics, 2021, 86, MR235-MR245.	2.6	9
44	Energy dissipation of P- and S-waves in fluid-saturated rocks: An overview focusing on hydraulically connected fractures. Journal of Earth Science (Wuhan, China), 2015, 26, 785-790.	3.2	8
45	Nonlinear rock-physics inversion using artificial neural network optimized by imperialist competitive algorithm. Journal of Applied Geophysics, 2018, 155, 138-148.	2.1	8
46	Laboratory measurements of seismic attenuation and Young's modulus dispersion in a partially and fully waterâ€saturated porous sample made of sintered borosilicate glass. Geophysical Prospecting, 2018, 66, 1384-1401.	1.9	7
47	Sparse Bayesian linearized amplitudeâ€versusâ€angle inversion. Geophysical Prospecting, 2019, 67, 1745-1763.	1.9	5
48	Hydro-mechanical coupling in porous rocks: hidden dependences to the microstructure?. Geophysical Journal International, 2020, 224, 973-984.	2.4	5
49	Numerical study of fracture connectivity response in seismic wavefields. , 2017, , .		4
50	Fluid pressure diffusion in fractured media: the role played by the geometry of real fractures. Journal of Geophysical Research: Solid Earth, 2021, 126, e2021JB022233.	3.4	4
51	Frequency-dependent attenuation in water-saturated cracked glass based on creep tests. Geophysics, 2017, 82, MR89-MR96.	2.6	3
52	Seismic Attenuation in Realistic Fracture Networks. , 2017, , .		3
53	Viscoelastic substitute models for seismic attenuation caused by squirt flow and fracture leak off. Geophysics, 2019, 84, WA183-WA189.	2.6	3
54	Modeling Seismic Attenuation Due to Wave-Induced Fluid Flow in the Mesoscopic Scale to Interpret Laboratory Measurements. , 2013, , .		2

#	Article	IF	CITATIONS
55	Velocity and attenuation characteristics of P-waves in periodically fractured media as inferred from numerical creep and relaxation tests. , 2014, , .		2
56	Forced oscillation measurements of seismic attenuation in fluid saturated sandstone. Acta Geophysica, 2017, 65, 165-172.	2.0	2
57	Numerical Analysis of Laboratory Attenuation Measurements. , 2017, , .		2
58	Squirt flow in porous media saturated by Maxwell-type non-Newtonian fluids. Physical Review E, 2021, 103, 023101.	2.1	2
59	Representative elementary volumes for evaluating effective seismic properties of heterogeneous poroelastic media. Geophysics, 2016, 81, D21-D33.	2.6	2
60	Seismic wave attenuation in fluid-saturated rock as result of gas dissolution. , 2014, , .		2
61	A simple hydro-mechanical approach to simulate squirt-type flow at any scale. , 2015, , .		2
62	Seismic wave attenuation in rocks saturated with bubbly liquids: Experiments and numerical modeling. , 2015, , .		2
63	Numerical assessment of local versus bulk strain measurements to quantify seismic attenuation in partially saturated rocks. , 2018, , .		2
64	Mass transfer between fluids as a mechanism for seismic wave attenuation: experimental evidence from water–CO2 saturated sandstones. Geophysical Journal International, 2022, 230, 216-234.	2.4	2
65	"Low-frequency reflections from a thin layer with high attenuation caused by interlayer flow,― GEOPHYSICS, 74, no. 1, N15–N23. Geophysics, 2009, 74, Y7-Y7.	2.6	1
66	Synchrotron-based X-ray tomographic images and segmentation techniques to account for effects of grain contacts and micro-cracks on rock properties. , 2013, , .		1
67	Laboratory measurements of seismic attenuation in water-saturated porous borosilicate. , 2014, , .		1
68	Attenuation in Fluid-Saturated Fractured Porous Media—Quasi-Static Numerical Upscaling and Wave Propagation Modeling. , 2017, , .		1
69	Frequencyâ \in dependent reflections from a layer with attenuation caused by interlayer flow. , 2009, , .		1
70	Effects of crack roughness on attenuation caused by squirt flow in Carrara marble. , 2020, , .		1
71	Numerical and laboratory measurements of seismic attenuation in partially saturated rocks. , 2012, , .		Ο
72	Synchrotron-based X-ray tomographic images: Raw data, segmentation techniques, and their influence		0

on estimated rock properties. , 2013, , .

#	Article	IF	CITATIONS
73	Interpreting attenuation in partially saturated sandstone using measurements of local fluid pressure and numerical modeling of fluid flow in poroelastic media. , 2013, , .		0
74	Laboratory apparatuses for measuring seismic attenuation in fluid-saturated rocks. , 2013, , .		0
75	Effects of fracture connectivity on S-wave attenuation caused by wave-induced fluid flow. , 2013, , .		0
76	Low-Frequency Elastic Properties of a Polymineralic Carbonate: Laboratory Measurement and Digital Rock Physics. Frontiers in Earth Science, 2021, 9, .	1.8	0
77	An accurate analytical model for squirt flow considering simple pore geometry. , 2021, , .		0
78	Sâ \in wave attenuation caused by waveâ \in induced fluid flow. , 2011, , .		0
79	S-wave attenuation caused by wave-induced fluid flow. , 2011, , .		0
80	Measuring and modeling transient fluid pressure in a partially saturated rock sample. , 2012, , .		0
81	Modeling seismic attenuation due to wave-induced fluid flow in the mesoscopic scale to interpret laboratory measurements. , 2013, , .		0
82	Laboratory-based seismic attenuation in Fontainebleau sandstone: Evidence of squirt flow. , 2015, , .		0
83	Laboratory measurements of seismic wave attenuation in Berea sandstone as a function of water saturation and confining pressure. , 2015, , .		0
84	Seismic attenuation of saturated cracked glass: Numerical analyses of experimental creep tests. , 2016, , .		0
85	P-wave modulus dispersion and attenuation caused by squirt flow in cracks with rough walls. , 2019, ,		0
86	Numerical study of dispersion and attenuation caused by squirt flow. , 2019, , .		0